Proceedings of the 7th International Conference on HydroScience and Engineering

Philadelphia, USA September 10-13, 2006 (ICHE 2006)

ISBN: 0977447405

Drexel University

College of Engineering

2DV HYDRODYNAMICS OF EMERGED RUBBLE-MOUND BREAKWATERS

Evangelos Koutandos[1], Panayiotis Prinos[2] and Christofer Koutitas[2]

ABSTRACT

In the present study the 2DV hydrodynamic characteristics of emerged rubble-mound breakwaters with or without overtopping is studied numerically using the Cornell Breaking waves and Structure (COBRAS) model, Liu et al. (1999), Liu et al. (2000), Garcia et al. (2004). The COBRAS model solves the 2DV Reynolds Averaged Navier-Stokes (RANS) equations, based on the decomposition of the instantaneous velocity and pressure fields into mean and turbulent quantities. Reynolds stresses are closed with an algebraic non-linear k-ε turbulence model, which can solve anisotropic–eddy-viscocity turbulent flows. The flow in the porous structure is described in the COBRAS model by the Volume-Averaged Reynolds Averaged Navier-Stokes (VARANS) equations, obtained by integration of the RANS equations in a control volume larger than the pore structure but smaller than the characteristic length scale of the flow. Another set of k-ε equations similar to the previous one is used to model turbulence production-dissipation within the porous medium, Hsu et al. (2002).

Two characteristic cases are examined numerically: (A) emerged breakwater without overtopping and (B) emerged breakwater with overtopping. In both cases numerical results, concerning the free surface evolution along the wave flume, are compared satisfactorily against experimental results from the European Project Delos. The 2DV hydrodynamic characteristics are revealed concerning the 2DV velocity and turbulence kinetic energy fields before, over and after the structure and the main differences between the two cases examined numerically are discussed. It is revealed that overtopping has a crucial effect in the mean field (velocity field), since much higher maximum velocities are observed mainly in the front upper part of the structure in the overtopping case and (B) in the turbulence field (turbulence kinetic energy field) since much higher maximum values are observed not only in the front upper part of the structure in the overtopping case but also in the porous body of the structure. These facts are mainly due to the stronger wave-structure interaction and the more intense momentum exchange through the water-porous material interface in the case of overtopping. Thus it is evident that overtopping can cause severe damages mainly in the front part but also in the core of emerged rubble-mound breakwaters due to the increased turbulence intensity.

Keywords: rubble mound breakwaters, overtopping

[1] Research Associate, Institute of Applied and Computational Mechanics, Foundation of Research and Technology, P.O. Box 1385, 71110, Heraklion Crete, Greece (ekoutant @iacm.forth.gr).
[2] Professor, Division of Hydraulics, Department of Civil Engineering Aristotle University, Thessaloniki, PC 54638, Greece (prinosp@civil.auth.gr, koutitas@civil.auth.gr).

1. INTRODUCTION

Rubble mound breakwaters are primarily designed to reduce wave loads on the coast through a series of wave transformation processes on and inside the structure. The relative importance of each one of the physical processes that take place in the interaction of a wave train with a rubble mound breakwater depends on the wave parameters (height, period, relative depth) and on the rubble mound characteristics (geometry, porosity, permeability). When the incident wave train impinges on the structure, part of the energy is reflected back to the sea, a part is dissipated and a part is transmitted in the leeside zone. Most of the incident wave energy is lost on the structure seaward slope, essentially by breaking. Part of the energy is also dissipated by air entrainment and friction at the solid skeleton interface and within the porous medium. For non-breaking waves, the flow resistance in the porous medium is the main dissipation mechanism. Significant non-linear interactions occur in the area of the structure between the various wave phases and some energy is transferred from the fundamental wave frequency to higher harmonics. A great number of numerical investigations have been carried out in order to characterize the performance of permeable structures Sollit & Cross (1972), Madsen (1974), Vidal et al. (1988), Liu at al. (1999), Liu at al. (2000), Hsu et al. (2002), Requejo et al. (2002). Experimental studies are rather limited due to the multifold problems that appear such as: scale effects, expensive models, difficulties in measurements due to breaking waves, van Gent (1994), van Gent (1995), Losada et al. (1995), Ting et al. (2004).

In the present study the 2DV hydrodynamic characteristics of emerged rubble-mound breakwaters with or without overtopping is studied numerically using the Cornell Breaking waves and Structure (COBRAS) model, Liu et al. (1999), Liu et al. (2000), Garcia et al. (2004).

2. DESCRIPTION OF THE NUMERICAL MODEL

In the COBRAS wave model the Reynolds Averaged Navier-Stokes (RANS) equations are solved in a 2DV computational field. Turbulence closure is achieved using a non-linear k-ε type turbulence model. Free surface evolution is described using the VOF method (Hirt & Nichols, 1981). Direct numerical simulation in the porous medium (the body of the permeable breakwater) is practically impossible due to the random geometry of the porous structure ; therefore the flow in the porous medium must be described using an integrated form of the Navier-Stokes over a certain control volume (Volume-Averaged Reynolds Averaged Navier-Stokes-VARANS). This control volume is larger than the pore structure but smaller than the characteristic length of the flow (Hsu et al, 2002). Another set of k-ε equations similar to the previous one is used to model turbulence production-dissipation within the porous media.

The boundary conditions of the mean flow field consists of a non-slip condition at the solid boundaries and a zero stress condition at the free-surface, Liu & Lin (1997), Lin & Liu (1998). With respect to the turbulence field, a log-law distribution of the mean tangential velocity in the turbulent boundary layer is considered near the solid boundary, where the values of k and ε can be expressed as functions of the distance from the solid from the solid boundary and the mean tangential velocity outside the viscous sublayer. On the free surface, the zero gradient boundary conditions for both k and ε are based on the assumption of no turbulence exchange between the air and water. The initial condition consists of a still water situation. The wave model includes a procedure of wave generation using an internal wave maker. The method consists of introducing a source function in the continuity equation for a group of cells defining the source region. The free surface above the source region responds to a pressure increment defined within the source region cells, and a train of surface gravity waves is generated (Lin & Liu, 1999). A sponge-layer method, (Israeli & Orszag, 1981), is used to absorb the waves that propagate in the direction opposite the zone of interest, with an imposed exponential damping law.

The computational domain in the wave model is discretized in rectangular cells. The computing mesh can be divided into submesh regions, which allows a variable cells spacing: a finer grid can be defined for the representation of specific study zones. The free surface is tracked using the Volume of Fluid (VOF) method developed by Hirt & Nichols (1981) that identifies the free surface location tracking the density change in each cell. Besides, the model allows the definition of flow obstacles using a partial cell treatment. The Reynolds equations are solved using a finite differences two-step projection method, Chorin (1968, 1969).

3. GOVERNING EQUATIONS

The RANS equations that describe the flow in the region outside the porous structure are the classical continuity and momentum equation, (Rodi, 1980).
The VARANS equations that describe the flow in the porous medium are the following (Hsu et al., 2002).

Continuity equation:

$$\frac{\partial < U_i >}{\partial x_i} = 0 \tag{1}$$

Momentum equation:

$$(1+C_A)\frac{\partial\langle U_i\rangle}{\partial t} + < U_j > \frac{\partial\langle U_i\rangle}{\partial x_j} = \left[-\frac{1}{\rho}\frac{\partial\langle P\rangle}{\partial x_i} - \frac{\partial\langle\overline{u_i u_j}\rangle}{\partial x_j} + \frac{1}{\rho}\frac{\partial\langle\tau_{ij}\rangle}{\partial x_j} + g_i\right]$$
$$-\left[a_1\langle U_i\rangle + a_2(< U_j >< U_j >)^{1/2}\langle U_i\rangle\right] \tag{2}$$

where the capitals letters denote the ensemble average and the non capitals represent turbulent fluctuations with respect to the ensemble mean. The Darcy's volume averaging operator, <>, is defined as $\langle a\rangle = \frac{1}{V}\int_{V_f} a dV$ where V denotes the total averaging volume, and V_f is the portion of V that is occupied by the fluid, which differs from the intrinsic averaging operator ,$<>^f$, defined by $\langle a\rangle^f = \frac{1}{V_f}\int_{V_f} a dV$. The relationship between the Darcy's volume averaging and intrinsic volume averaging is $\langle a\rangle = n\langle a\rangle^f$ where n is the porosity ($n = V_f / V$). C_A denotes the added mass coefficient ($C_A = \gamma_p(1-n)/n$, γ_p=0.34) and n is the porosity. The last two terms in equation (2) are known as Darcy and Forchheimer terms respectively.

Coefficients a_1 and a_2 are calculated from the following relationships (Sollitt & Cross, 1972, Losada et al., 1995)

$$a_1 = \frac{\nu}{K}, \quad a_2 = \frac{C_f}{\sqrt{K}} \tag{3}$$

where ν is the water kinematic viscosity ($1.0\cdot10^{-6}$ m^2/sec), C_f a dimensionless coefficient and K the permeabitlity (m^2) provided by the following relationship (van Gent, 1994, 1995) :

$$K = \frac{D_{50}^{2} \cdot n^{3}}{\alpha(1-n)^{2}} \tag{4}$$

where D_{50} is the mean diameter of the porous material and α an empirical coefficient.
According to van Gent (1995) for the calculation of C_f (equation 3) the following relationship is proposed:

$$C_f = \beta \frac{1-n}{n} \frac{\sqrt{K}}{D_{50}} \tag{5}$$

where β is an empirical coefficient.

Several researchers (Madsen, 1974, Vidal et al., 1988, van Gent, 1995) have proposed values for the coeeficients α, β and γ according the material and the length scale. Liu et al. (1999) have used values γ_p=0.34, α=200, β=1.1. This approach is followed in the present work. In the regions outside the porous material where n=1 and C_A=0 the VARANS equations return to the original RANS equations.

4. THE EXPERIMENTAL PROGRAM

The available experimental results come from the European Research Program DELOS. The experiments were conducted in the Cantabria University aiming at a thorough study of the hydrodynamics of low crested permeable rubble mound breakwaters. The experimental layout in the Cantabria University wave flume is presented in Figure 1.

The wave flume is 24.05 m long, 0.60 m wide and 0.80 m deep. The wavemaker and the wave reflection absorption system occupy an area 4 m long in the left end of the flume. The following 4 m are occupied by a false bottom that can be partially or totally removed to set off a current in the flume. The remaining 16 m of the flume are available for testing of models. The length of the crest of the examined breakwaters models was 1 m and the slopes 1V/2H. The height of the crest was 20 cm from the flume bed, or 30 cm above the false bottom. On the front face of the of the rubble mound structure, a plexiglass ramp with a 1V/20H slope connected to the false bottom with the bottom of the flume. In the lee, another 8 m 1V/20H plexiglass ramp was used to simulate the rear beach and act as an energy dissipater to minimize the influence of reflected waves on results.

The experimental equipment consisted of a number of wave gauges, pressure and velocity sensors. The layout of the experimental equipment is presented in Figure 1.

5. NUMERICAL SIMULATIONS

Two different cases were examined numerically, one without wave overtopping (T=1.6 sec & H_i=5 cm) and one with wave overtopping (T=1.6 sec & H_i=10 cm). The water depth in both cases was 30 cm and therefore the emerged height of the structure 0.05 cm. The porosity of the breakwater was in both cases 0.53. The length of the base of the structure was 2 m while the length of the crest 1 m. The computational mesh, Figure 2, consisted of 4 subregions with dx (horizontal resolution) from 0.04 m to 0.01 m in the region of the structure. Dy (vertical resolution) was constant in all subregions equal with 0.01 m. Dt (time-step) in all numerical experiments was set equal to 0.0025 sec while the total time of each numerical experiment was 80 sec. Several grids have been employed to test the grid dependency of the results. It is found that the same results are obtained for the water surface elevation and the velocity field even if a coarser grid is used. This is not the case for the turbulent quantities for which the grid dependency is stronger. For the grid employed the results for both the mean and the turbulence quantities are considered grid independent. Results presented are from 30 T for which numerical stability is achieved, indicated by the total mass and energy in the domain.

6. NUMERICAL RESULTS-ANALYSIS

In this section numerical results are presented and analyzed especially comparing the numerical and experimental results concerning the free surface evolution, from the two cases examined. 2DV wave velocity and turbulent kinetic energy fields from the numerical simulations are also presented for all cases.

In Figure 3 a comparison is presented concerning the free surface evolution in wave gauge 3 (upstream the breakwater), wave gauge 6 (in the porous body of the breakwater) and wave gauge 9 (downstream the breakwater) for the non overtopping case. The corresponding graph for the overtopping case is presented in Figure 4. It is observed that in both cases only a small percentage of the incident wave energy passes through the porous body of the breakwater due to breaking and energy dissipation due to flow resistance in the porous medium. In both cases the performance of the wave model is satisfactory.

In Figures 5 and 6, the 2DV velocity fields for T=1.6 sec, H_i=5 cm (non overtopping case) and T=1.6 sec, H_i=10 cm (overtopping case) are presented. It is noted that maximum wave velocities that appear in the second case where overtopping occurs are almost triple the corresponding wave velocities for the non overtopping case despite the fact that the wave height is double in value in the second case. The maximum velocity area is the seaward slope of the structure.

In Figures 7 and 8, the 2DV turbulent kinetic energy fields for T=1.6 sec, H_i=5 cm (non overtopping case) and T=1.6 sec, H_i=10 cm (overtopping case) are presented. Maximum values that appear in the second case where overtopping occurs are almost 2.5 times the corresponding values for the non overtopping case .The area of maximum values is the upper part of the seaward slope of the structure near the crest, where the main interaction of the incident waves with the structure takes place, indicating maximum energy dissipation due to the developing turbulence. On the contrary on the landward slope of the structure developing turbulence is of minor importance.

These facts are mainly due to the stronger wave-structure interaction and the more intense momentum exchange through the water-porous material interface in the case of overtopping. Thus it is evident that overtopping can cause severe damages mainly in the front part but also in the core of emerged rubble-mound breakwaters due to the increased turbulence intensity.

7. CONCLUSIONS

In the present study the 2DV hydrodynamic characteristics of emerged rubble-mound breakwaters with or without overtopping was studied numerically. Available experimental results from the European Program Delos were compared with numerical results obtained with the use of the COBRAS wave model. Detailed computed velocities and turbulence kinetic energy in the vicinity of the structure for the overtopping and non-overtopping cases reveal the main differences between the two cases. The following conclusions can be derived:

(a) It is observed that in both cases (overtopping and non overtopping) only a small percentage of the incident wave energy passes through the porous body of the breakwater due to breaking and energy dissipation due to flow resistance in the porous medium.

(b) It is noted that maximum wave velocities that appear in the second case where overtopping occurs are almost triple the corresponding wave velocities for the non overtopping case despite the fact that the wave height is double in value in the second case. The maximum velocity area is the seaward slope of the structure.

(c) Maximum values of turbulent kinetic energy that appear in the second case where overtopping occurs are almost 2.5 times the corresponding values for the non overtopping case .The area of maximum values is the upper part of the seaward slope of the structure near the crest, where the main interaction of the incident waves with the structure takes place, indicating maximum energy dissipation due to the developing turbulence. On the contrary on the landward slope of the structure developing turbulence is of minor importance.

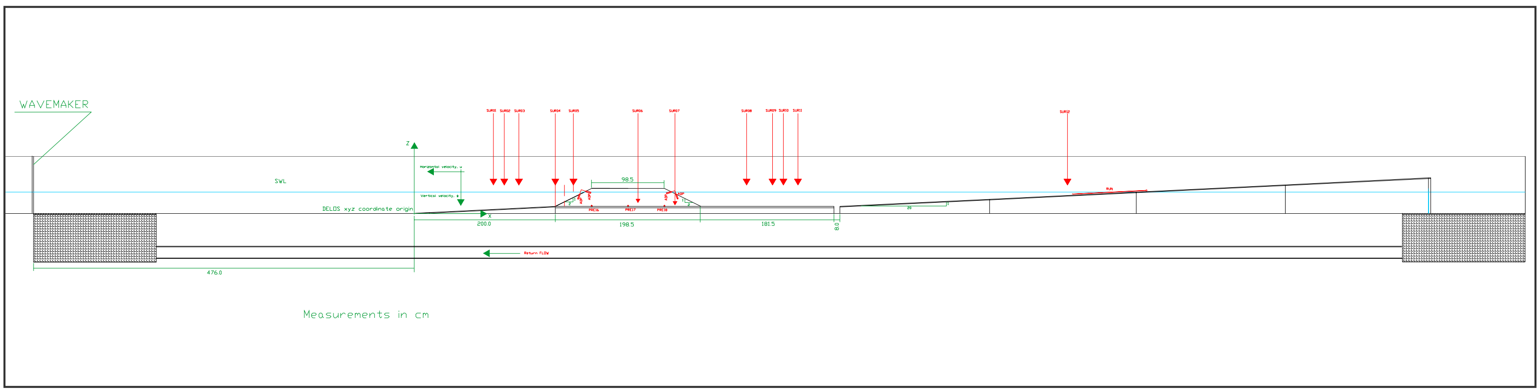

Figure 1 The experimental layout in the Cantabria University wave flume.

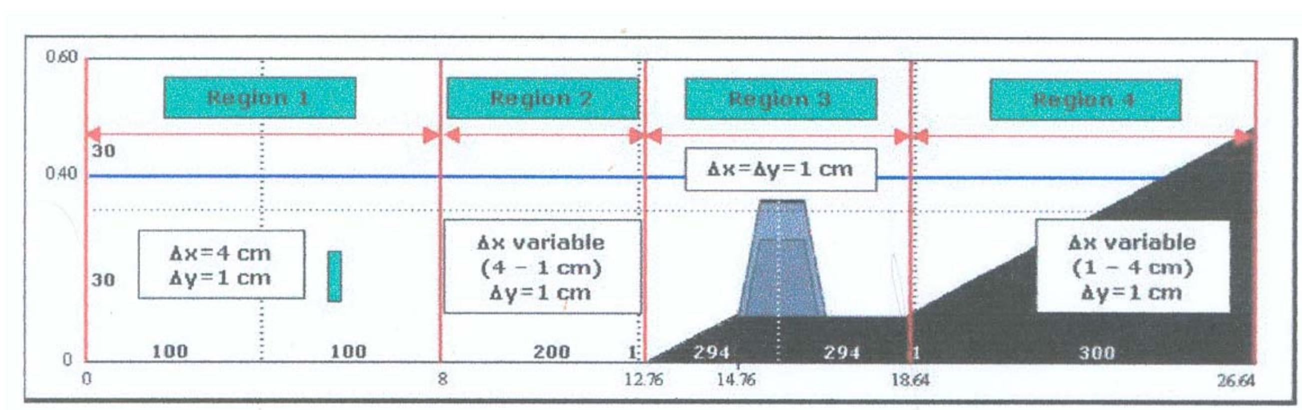

Figure 2 The computational domain.

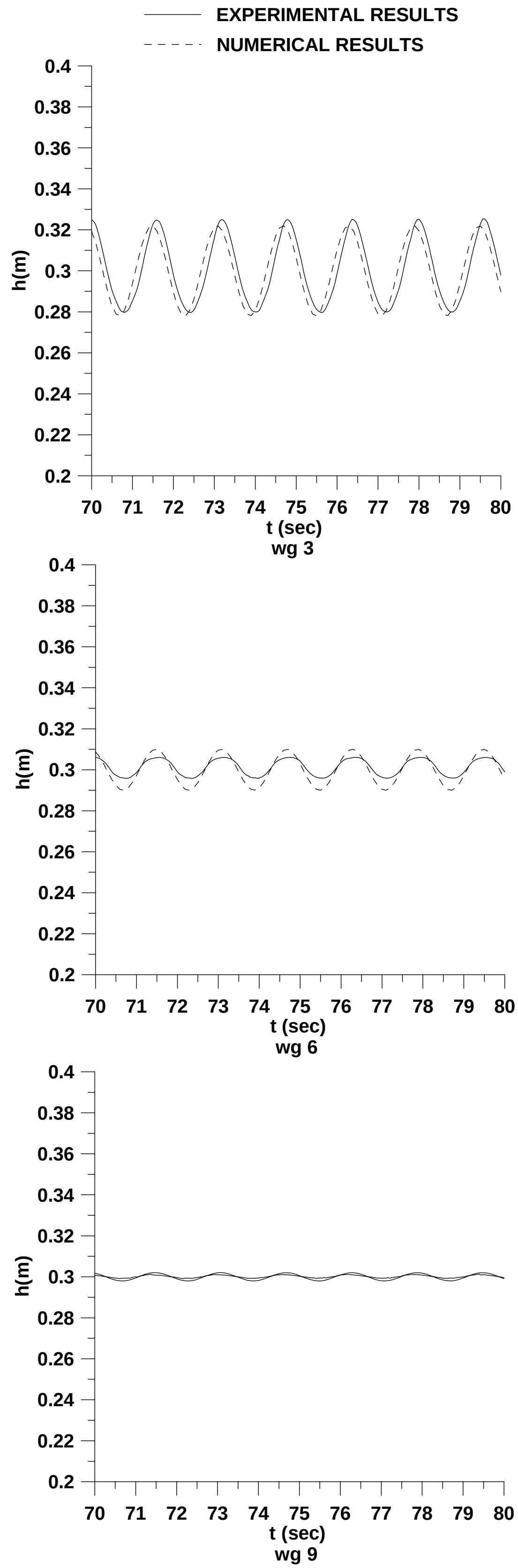

Figure 3. Numerical and experimental results comparison (without overtopping-T=1.6 sec & H_i=0.05m).

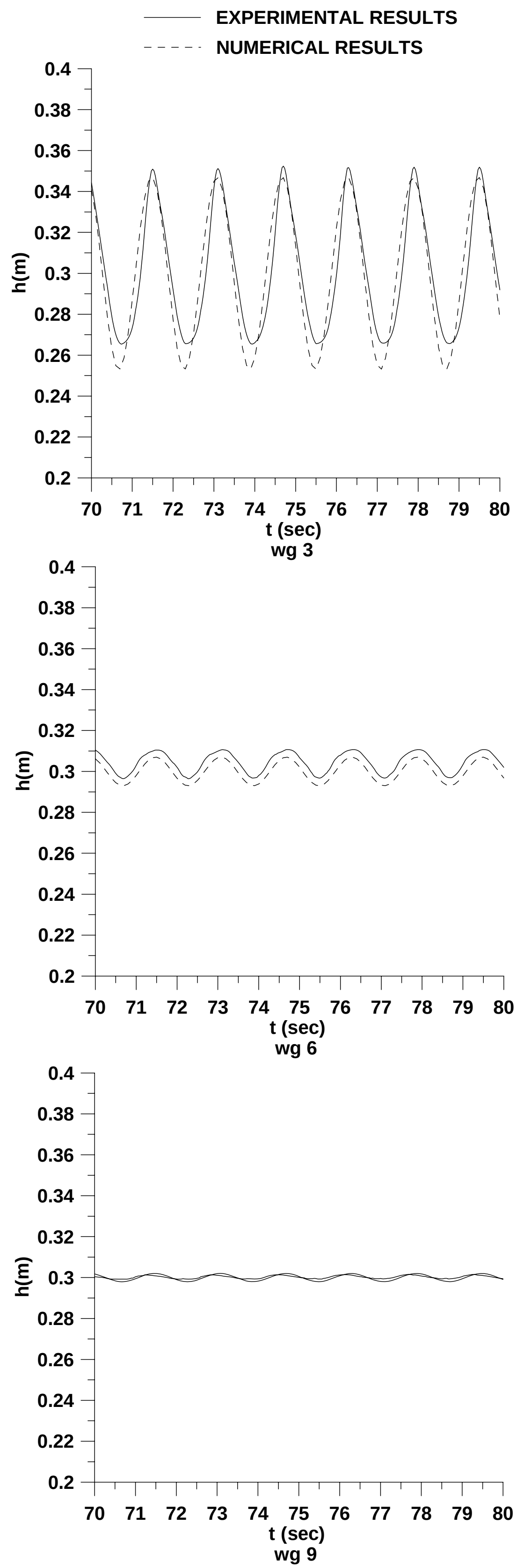

Figure 4. Numerical and experimental results comparison (with overtopping-T=1.6 sec & H_i=0.10 m).

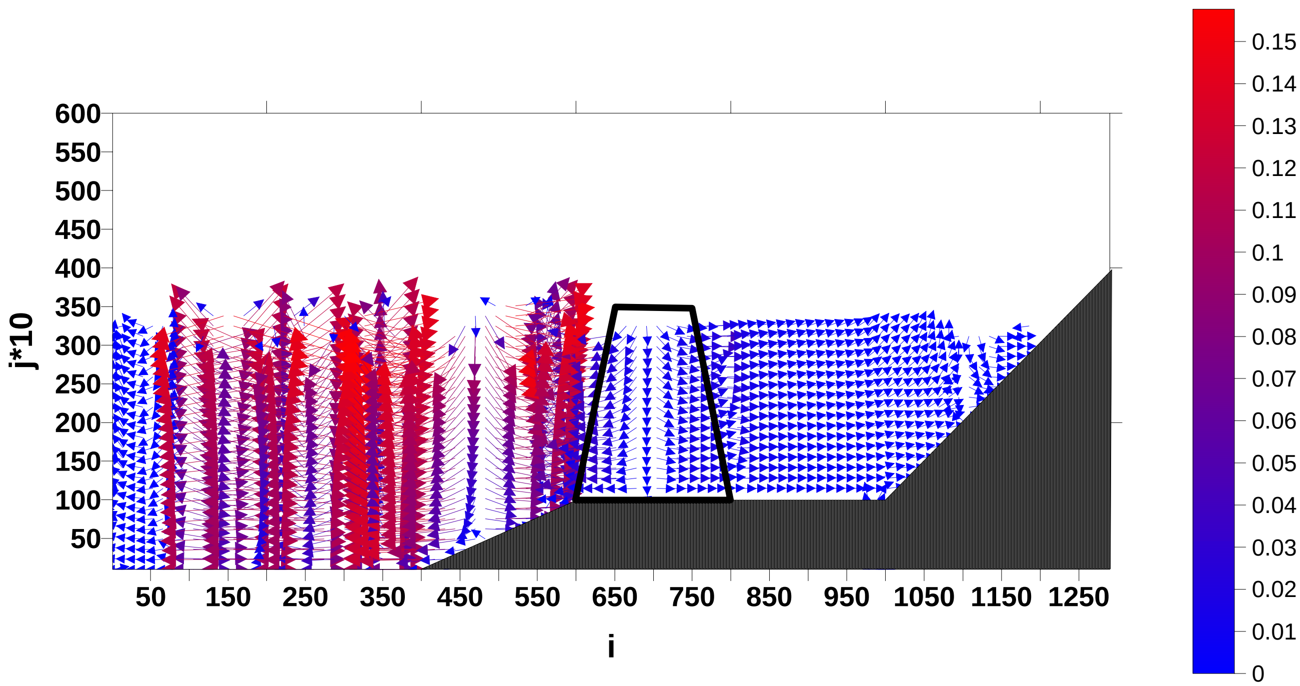

Figure 5. 2DV velocity field (without overtopping, T=1.6 sec & H_i=0.05 m).

.

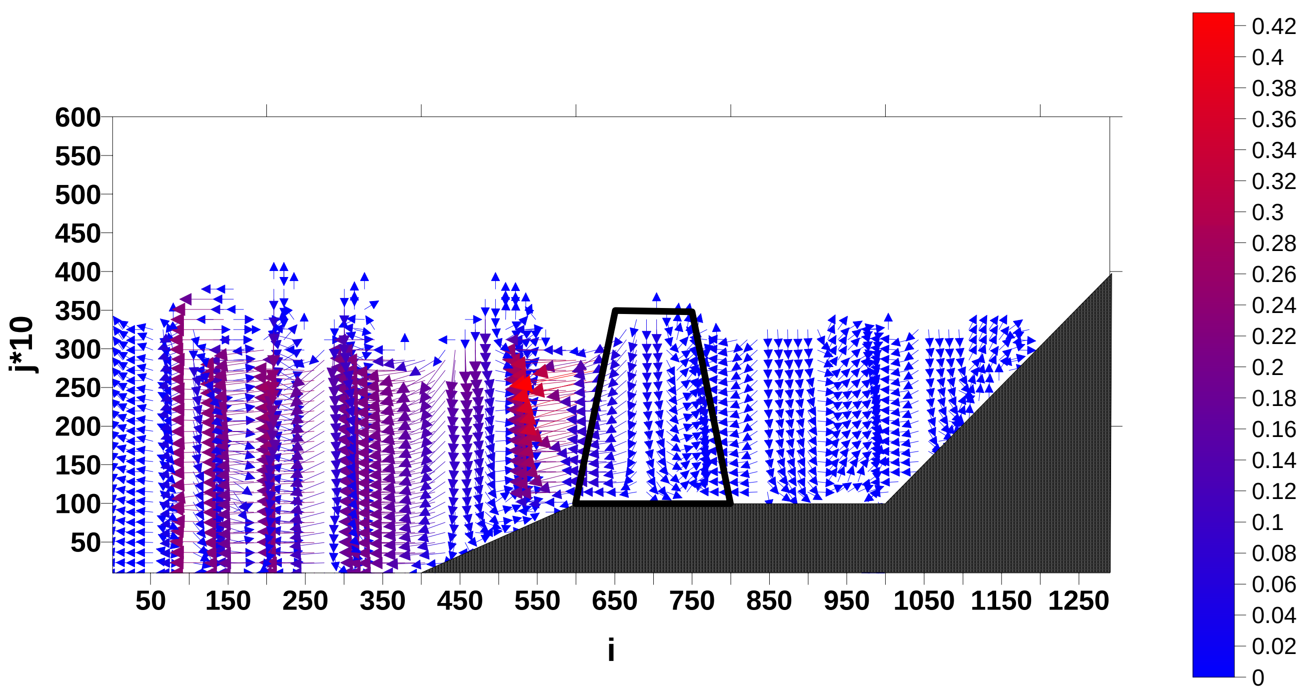

Figure 6. 2DV velocity field (with overtopping, T=1.6 sec & H_i=0.10 m).

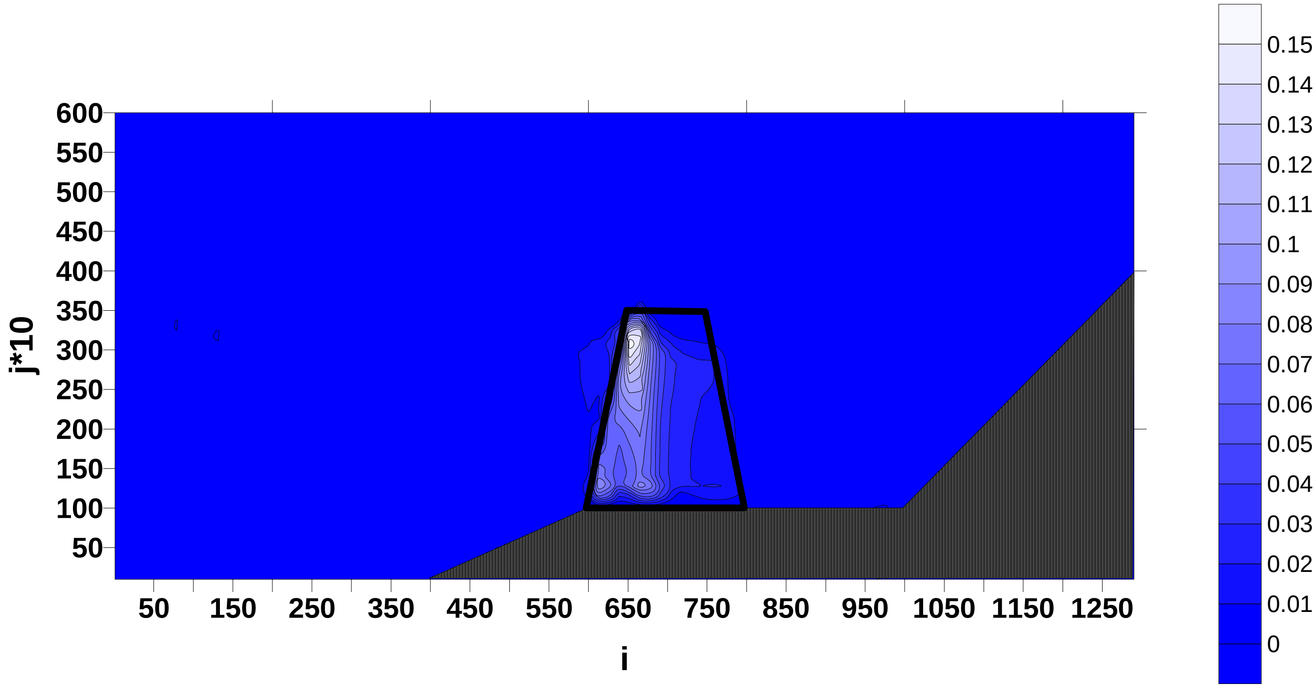

Figure 7. 2DV turbulent kinetic energy field (without overtopping, T=1.6 sec & H_i=0.05 m).

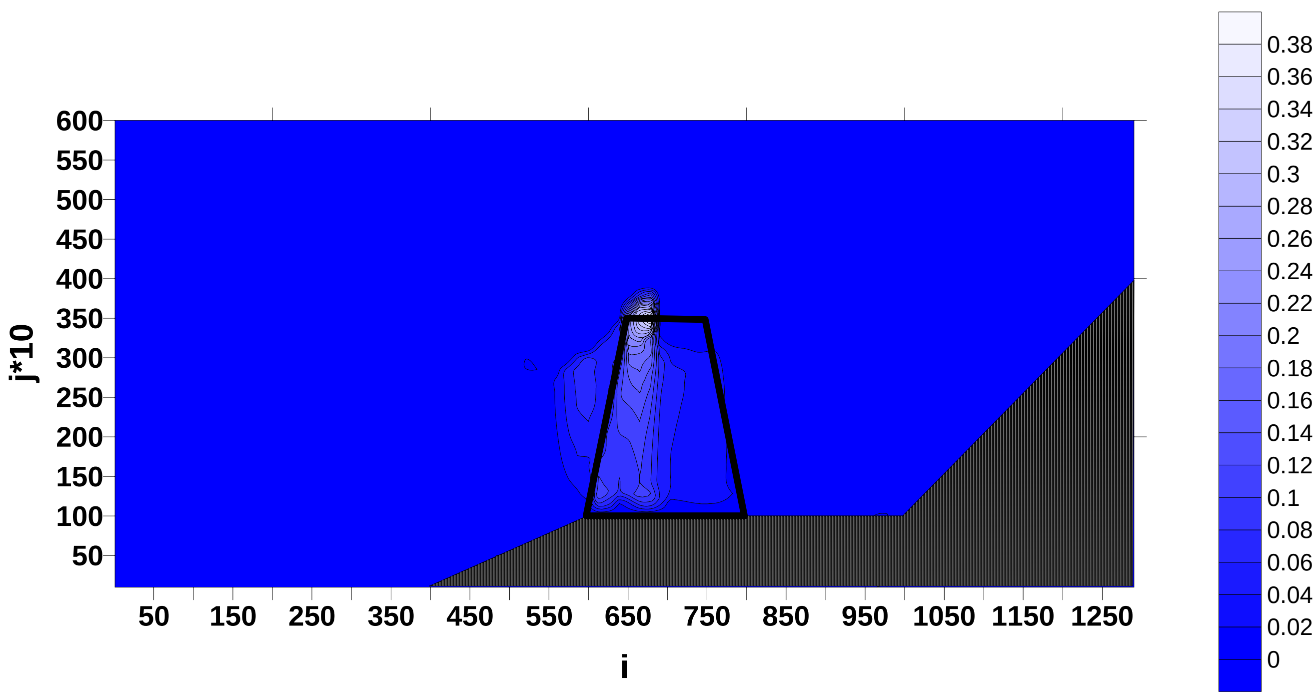

Figure 8. 2DV turbulent kinetic energy field (with overtopping, T=1.6 sec & H_i=0.10 m).

ACKNOWLEDGEMENT

The authors acknowledge the financial support through the program “PYTHAGORAS-I”, provided to the first author for conducting postdoctoral research.

REFERENCES

Chorin, A.J. 1968. Numerical solution of the Navier-Stokes equations. Math. Comp. 22, 745-762.
Chorin, A.J. 1969. On the convergence of discrete approximations of the Navier-Stokes equations. Math. Comp. 23, 341-353.
Garcia, N., Lara, J.,L., Losada, I., J., 2004. 2-D Numerical analysis of near-field flow at low – crested permeable breakwaters. Coastal Engineering 51, 991-1020.
Hirt, C.W., Nichols, B.D., 1981. Volume of Fluid (VOF) Method for the Dynamics of Free Boundaries. Journal of Computational Physics 39, 201-225.
Hsu, T. J., Sakakiyama, T., Liu, P.L.-F, 2002. A numerical model for wave motions and turbulence flows in front of a composite breakwater. Coastal Engineering 46,25-50.
Israeli, M., Orszag, S.A., 1981. Approximation of radiation boundary conditions. Journal of Computational Physics 41, 25-50.
Liu, L.-F. P., Lin, P., 1997. A numerical model for breaking waves : The Volume of Fluid Method. Research Report. No. CACR-97-02, Center for Applied Coastal Research, Ocean Engineering Laboratory, University of Delaware.
Lin, P., Liu, L.-F. P., 1998. A numerical study of breaking waves in the surf zone. Journal of Fluid Mechanics 359, 239-264.
Lin, P., Liu, L.-F. P., 1999. Internal wave-maker for Navier-Stokes equation models. Journal of Waterway, Port, Coastal and Ocean Engineering 125 (4), 207-215.
Liu, P.L.-F., Lin, P., Chang, K.A., Sakakiyama, T., 1999. Numerical modeling of wave interaction with porous structures. Journal of Waterway Port Coastal and Ocean Engineering 125, 322-330.
Liu, P.L.-F., Lin, P., Hsu, T., Chang, K., Losada, I.J., Vidal, C., Sakakiyama, T., 2000. A Reynolds averaged Navier-Stokes equation model for non linear water wave and structure interactions. Proc. Coastal Structures ‘99, 169-174.
Losada, I. J., Losada, M. A., Martín, A., 1995. Experimental study of wave-induced flow in a porous structure. Coastal Engineering, 26, 77-98.
Madsen, O. S., 1974. Wave transmission through porous structures. Journal of Waterway, Harbour, Coastal and Ocean Engineering, Div., ASCE, 100 (3), 169-188.
Requejo, S., Vidal, C., Losada, I.J., 2002. Modeling wave loads and hydraulic performance of vertical permeable structures. Coastal Engineering 46, 249-276.
Rodi, W., 1980. Turbulence Models and their Application in Hydraulics- A State of the Art Review. I.A.H.R. Publication, Delft, Netherlands.
Sollitt, C. K., Cross, R. H., 1972. Wave transmission through permeable breakwaters. In: Proceedings of 13th International Conference on Coastal Engineering, ASCE, New York, 1827-1846.
Ting, C.-L., Lin, M.-C., Cheng, C.-Y., 2004. Porosity effects on non-breaking surface waves over permeable submerged breakwaters, Coastal Engineering, Vol. 50, pp. 213-224.
van Gent, M. R. A., 1994. The modelling of wave action on and in coastal structures. Coastal Engineering, 22, 311-339.
van Gent, M. R. A., 1995. Wave interaction with permeable coastal structures. PhD Thesis, Delft University, Delft, The Netherlands.

Vidal, C., Losada, M. A., Medina, R., Rubio, J., (1988). Solitary wave transmission through porous breakwaters. In: Proceedings of 21st International Conference on Coastal Engineering, ASCE, New York, 1073-1083.